

Knee Kinematics Feature Selection for Surgical and Nonsurgical Arthroplasty Candidate Characterization

M. A. Ben Arous^{1,6}, M. Dunbar², S. Arfaoui^{3,6}, A. Mitiche⁵, Y. Ouakrim^{4,6}, A. Fuentes⁶,
G. Richardson² and N. Mezghani^{4,6}

¹Collège Bois de Boulogne, Montreal, Quebec, Canada

²Dalhousie University, Halifax, Nova Scotia, Canada

³Collège Jean-de-Brébeuf, Montreal, Quebec, Canada

⁴LICEF Research Center, TELUQ University, Montreal, Quebec, Canada

⁵INRS Énergie, Matériaux et Télécommunications, Montreal, Quebec, Canada

⁶Laboratoire de Recherche en Imagerie et Orthopédie (LIO), ETS/CRCHUM, Montreal, Quebec, Canada

Keywords: Knee Kinematic, Biomechanical Data, Feature Selection, Complexity Measures, Arthroplasty.

Abstract: The purpose of this study is to investigate a method to select a set of knee kinematic data features to characterize surgical vs nonsurgical arthroplasty subjects. The kinematic features are generated from 3D knee kinematic data patterns, namely, rotations of flexion-extension, abduction-adduction, and tibial internal-external recorded during a walking task on a dedicated treadmill. The discrimination features are selected using three types of statistical complexity measures: the Fisher discriminant ratio, volume of overlap region, and feature efficiency. The interclass distance measurements which the features thus selected induce demonstrate their effectiveness to characterize surgical and nonsurgical subjects for arthroplasty.

1 INTRODUCTION

Knee kinematic data during locomotion, which can be easily acquired in clinical settings (Lustig et al., 2012), provide useful information about knee function and can serve the development of objective methods of computer aided diagnosis to assist surgical decisions and treatment.

Preoperative knee conditions, prosthesis design, and surgical techniques all influence knee kinematics following an arthroplasty. However, kinematic studies have primarily focused on postoperative knee kinematics (Seon et al., 2011). Preoperative investigations have been scarce (Casino et al., 2009; Casino et al., 2008; Mihalko et al., 2007) in great part due to knee kinematic data complexity (Mezghani et al., 2008), which are high-dimensional vectors and of high variability. The studies in (Casino et al., 2009; Casino et al., 2008; Mihalko et al., 2007) investigated knee kinematic data of osteoarthritis patients and (Mezghani et al., 2016) specifically addressed surgical vs nonsurgical discrimination of candidates for arthroplasty.

High kinematic data variability and

dimensionality are illustrated in Figure 1, which shows the graph of a sample of one hundred fifty-three (153) participants curves and their average curves. The intra-class high variability and inter-class proximity, which are evident in the figure, make discriminating feature extraction notoriously difficult. In spite of the importance of this problem, there has been no investigation of feature extraction in terms of objective metrics. By reducing the dimension of the data representation vector, feature selection affords a means of escape from the curse of dimensionality while maintaining a good description of the data. The feature selection methods are usually evaluated using the classification rate of a chosen classifier. However, these methods are classifier dependent. Our goal is to investigate measures for feature selection independent of classifiers design.

In this study, we propose a knee kinematics feature selection method based on statistical complexity measures, namely, the *Fisher discriminant ratio*, *volume of overlap region*, and *feature efficiency*. The purpose is to select the most discriminant features from a feature set of interest in a classification task.

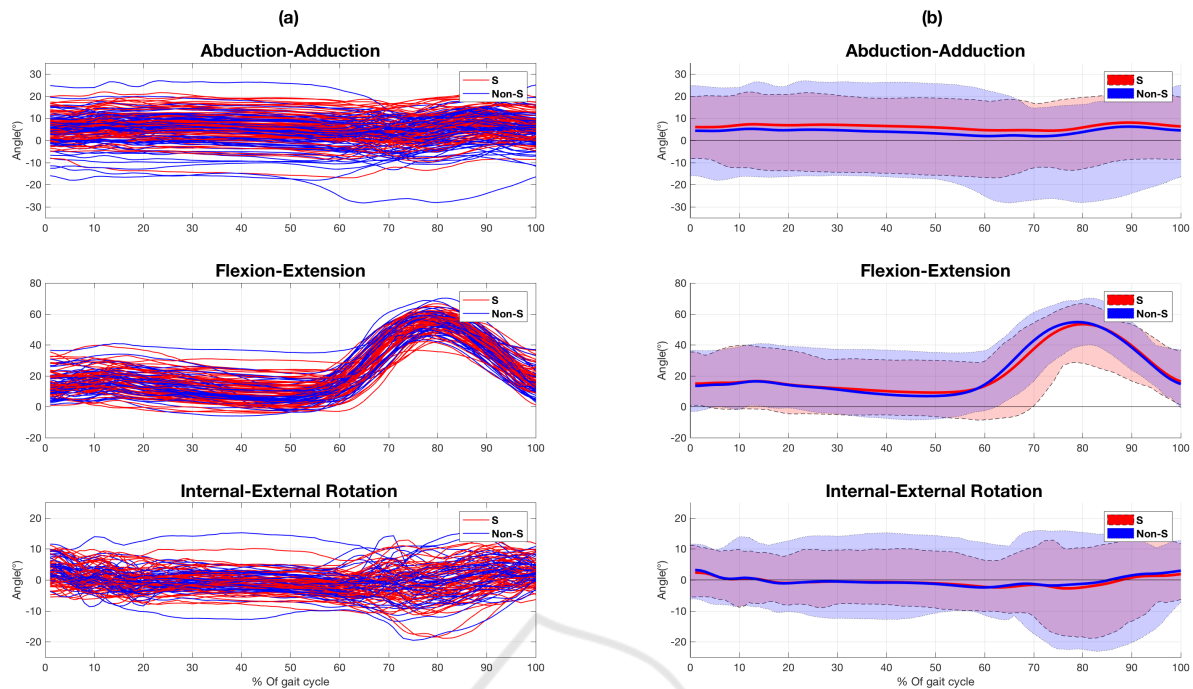


Figure 1: (a) Kinematic gait signals (of the database) during a gait cycle: Abduction-adduction (line1), Flexion-extension (line 2), and Internal-external rotation (line3). The signals were interpolated and resampled from 1% to 100% (100 points) of the gait cycle. Each red curve represents a surgical participant (S) and each blue one represent a Non-Surgical (Non-S) participant (b) The mean and standard deviation of the kinematic gait signals. The blue and red lines represent respectively the S and Non-S group average patterns.

2 METHODS

2.1 Database

The database was provided by the Division of Orthopedic Surgery in Halifax QEII Health Sciences Center (Nova Scotia, Canada). The one hundred fifty-three (153) participants enrolled for the research had a diagnosis of knee osteoarthritis ranging from moderate to severe condition and were all scheduled for an arthroplasty consult. All participants also went through an orthopedic physical assessment by one of two experienced orthopedic surgeon and were consequently assigned to surgical (S) or nonsurgical (Non-S) groups. Table 1 summarizes the principal demographic characteristics of the participants. A t-test was performed to examine the general participant characteristic differences between the two groups. The statistical analysis was conducted using SPSS 20.0 (Statistical Package for Social Sciences). The P-value of 0.05 was set as level of statistical significance.

All participants underwent physiotherapy assessment and patients reported outcome questionnaires. Three-dimensional (3D) knee

Table 1: Demographic characteristics of S and Non-S groups (BMI design the mean body mass index).

	Groupe S N =80	Groupe Non-S N = 73
Age (year)	64,7 ± 9,3	64.2 ± 9.2
Height(m)	1.67 ± 0.1	1.69 ± 0.1
Weight (kg)	92.8 ± 23.7	90.9 ± 19.3
BMI (kg / m ²)	33.13 ± 7.0	31.5 ± 6,0
Proportion of men / group	37%	50%

kinematics data, namely, rotation measurements for flexion-extension, abduction-adduction, and tibial internal-external, in the sagittal, frontal, and transverse planes, respectively, were recorded while each participant walked on a treadmill at a self-selected, comfortable speed. A validated knee marker attachment system, the KneeKG system (Emovi Inc, Montreal, Canada) (Figure. 2), was installed on the participant's knee to record the 3D kinematics data during gait trials of 45 sec on an instrumented treadmill at a comfortable self-speed.

This motion capture device is composed of a harness and a tibial plate fixed quasi rigidly onto

the femoral condyles and tibial crest, and provides accurate, repeatable, and reliable measurements (Lustig et al., 2012). A number of representative gait cycles, generally 15, were averaged to obtain a means pattern per subject. This was followed by interpolation and resampling from 1% to 100% of the gait cycle, therefore giving 100 measurement points for each participant (Figure. 1).



Figure 2: Knee kinematic acquisition system.

2.2 Kinematic Feature Extraction

Sixty-nine (69) biomechanical parameters were extracted from the 3D kinematic signals. These were chosen from the common variable in clinical biomechanical studies of knee osteoarthritis populations (Asthephen et al., 2011; Bytyqi et al., 2014; Mezghani et al., 2017), such as maxima, minima, varus and valgus thrusts, angles at initial contact, mean value and range of motion (ROM) throughout gait cycles, and sub-phases (stance phase, swing phase) as illustrated in Figure 3.

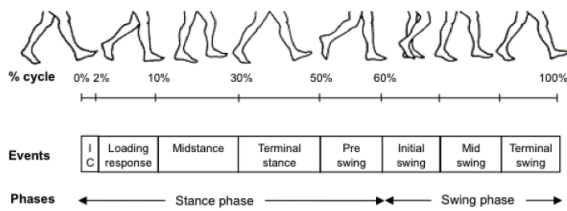


Figure 3: Gait cycle phases and sub-phases.

2.3 Kinematic Feature Selection using Statistical Measures of Complexity

Statistical measures of complexity, which evaluates class ambiguity, were used to afford an evaluation

of the discriminant power of the class representation features, i.e., the features capacity to distinguish data samples from distinct classes. For each individual feature, the complexity measure examines the range and spread of the values of instances of different classes and verify the discriminant power of a single feature.

Let $\mathcal{D} = \{x_1, x_2, \dots, x_n\}$ a data set containing n elements, each belonging to one of two distinct classes c_1 and c_2 . In our case, c_1 corresponds to the surgical group (S) and c_2 to nonsurgical group (Non-S). Each element x is characterized by a feature vector (f_1, f_2, \dots, f_p) , where p is the dimension of the feature space ($p = 69$ biomechanical parameters).

The overlap is evaluated according to the following measures:

2.3.1 Fisher Discriminant Ratio (F1)

This measure computes the maximum discriminative power of each feature. For a two-class data set, the Fisher discriminant ratio $F1(i)$ of a feature f_i , ($i = 1, \dots, p$), is defined as:

$$F1(i) = \frac{(\mu_{i1} - \mu_{i2})^2}{(\sigma_{i1}^2 + \sigma_{i2}^2)}, \quad (1)$$

where μ_{i1} , μ_{i2} , σ_{i1} , σ_{i2} are the means and variances of the two classes, respectively, according to the i^{th} feature, ($i = 1, 2, \dots, p$).

A high value of the Fisher's discriminant ratio indicates that the feature enables to separate the data set of different classes with partitions that are parallel to an axis of the feature space.

2.3.2 Volume of Overlap Region (F2)

This measure estimates the amount of relative overlap of the bounding regions of two classes (Lorena and de Souto, 2015). For each feature f_i , ($i = 1, \dots, p$), where p is the dimension of the feature space, the Volume of overlap region (F2) is defined as:

$$F2(i) = \frac{\text{MinMax}(i) - \text{MaxMin}(i)}{\text{MaxMax}(i) - \text{MinMin}(i)} \quad (2)$$

$$\text{MinMax}(i) = \min(\max(f_i, c_1), \max(f_i, c_2))$$

$$\text{MaxMin}(i) = \max(\min(f_i, c_1), \min(f_i, c_2))$$

$$\text{MaxMax}(i) = \max(\max(f_i, c_1), \max(f_i, c_2))$$

$$\text{MinMin}(i) = \min(\min(f_i, c_1), \min(f_i, c_2))$$

where f_i is the i -th feature. c_1 and c_2 refer to the two classes and $\max(f_i, c_i)$ and $\min(f_i, c_i)$ are, respectively, the maximum and minimum values of the feature f_i for class c_i . In other words, the volume

of overlap is evaluated using the ratio of the width of the overlap interval $\text{MinMax}(i) - \text{MaxMin}(i)$ to the width of the entire interval $\text{MaxMax}(i) - \text{MinMin}(i)$.

A low value of the volume of overlap region means that the feature can discriminate the examples of different classes.

2.3.3 Feature Efficiency (F3)

The feature efficiency measure is particularly relevant when dealing with high-dimensional data. It informs on how much each feature contributes to the separation of the classes. The contribution is called efficiency. For each feature, the ambiguous (overlapping) regions are removed so that only non-overlapping regions remain.

Let $\text{MinMax}_i = \min(\max(f_i, c_1), \max(f_i, c_2))$ and $\text{MaxMin}_i = \max(\min(f_i, c_1), \min(f_i, c_2))$. For each feature f_i , the feature efficiency $F3(i)$ is given by the following ratio:

$$F3(i) = \frac{|f_i \in [\text{MinMax}_i, \text{MaxMin}_i]|}{n}, \quad (3)$$

where $| \cdot |$ denotes the number of non-overlapping elements and n is the total number of elements in both classes.

2.3.4 Thresholds of Class Ambiguity Measures

To be used to select the discriminant feature, the class ambiguity measures require, for each measure, the estimation of a threshold to decide if a specific feature is whether discriminant or not.

We investigated thresholds estimation using the probability distribution of the class ambiguity measures. For each measure, i.e., the Fisher discriminant ratio $F1(i)$, the volume of overlap region $F2(i)$ and the feature efficiency $F3(i)$, a probability distribution has been determined. The thresholds are estimated using the 95th quantile of the probability distribution.

2.4 Evaluation of the Selected Features

Several studies have addressed feature selection evaluation. The methods of evaluation can be divided in two major groups: individual feature evaluation and feature subset evaluation. A subset evaluation is relevant in our case. We evaluated the efficiency of the selected feature subset using interclass distance. This measure was compared to the interclass distance using the original set of all features (consisting of 69 biomechanical features). A high value of the interclass distance indicates that the features are relevant.

3 RESULTS AND DISCUSSION

The class ambiguity measures of each feature taken individually and the corresponding thresholds are represented in Figure. 4. The thresholds are estimated using the 95th quantile of the probability distribution of each complexity measure as explained in the Section 2.3.4.

Table 2: Selected features.

Selected features
f_{12} : Minimum frontal plan angle during mid-stance, where abduction is negative and adduction is positive
f_{18} : Maximum axial plane angle, where internal rotation is negative and external rotation is positive
f_{21} : Maximum flexion angle during the loading phase
f_{26} : Mean adduction/adduction angle during the stance phase
f_{28} : Maximum flexion angle
f_{29} : % of GC where the maximum angle of flexion occurs
f_{38} : Maximum frontal plan angle, where abduction is negative and adduction is positive
f_{46} : Frontal plane angle at 54 % of the GC
f_{54} : Mean transverse plane rotation during the swing phase
f_{61} : Transverse plane rotation angle at the end of the terminal swing
f_{62} : ROM of the internal/external rotation
f_{63} : Maximum flexion angle (absolute value) during loading

Figure 4 (a) represents the discriminant ratio $F1(i)$ for each feature f_i ($i = 1, 2, \dots, 69$) computed according to Eq. 1. The threshold was set to 0.08. The selected feature set contains $\{f_{21}, f_{26}\}$. In Figure 4(b), we represented the ratio of the width of the overlap interval $F2(i)$ of each feature. The threshold here was set to 0.57 and we were interested in low values of $F2(i)$. The only retained feature is $\{f_{12}\}$. Finally, in Figure 4(c), we represented the individual feature efficiency which describes the ratio of the number of samples that are not in the overlapping region to the total number of samples. The threshold was set to 0.38. The combination of the features identified as a result of the complexity analysis forms the following set of the selected features are: $\{f_{18}, f_{26}, f_{28}, f_{29}, f_{38}, f_{46}, f_{54}, f_{61}, f_{62}, f_{63}\}$. Table 2

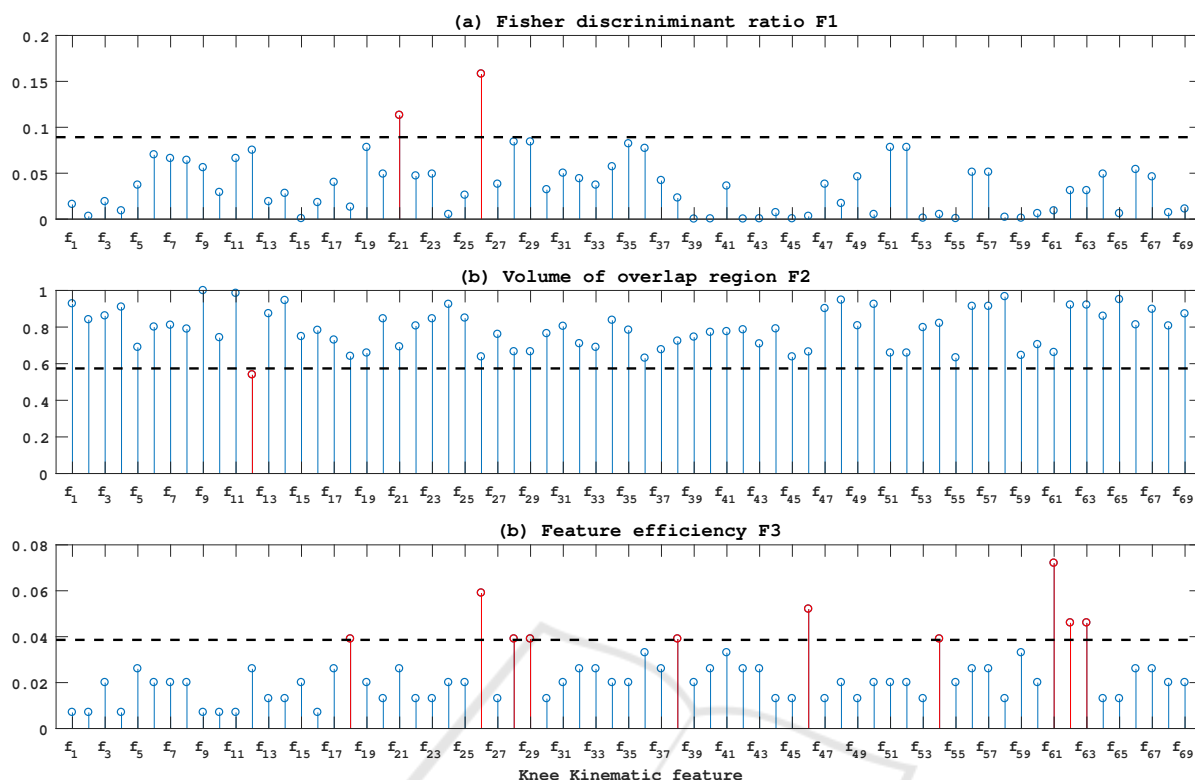


Figure 4: Measures of class ambiguity for each feature f_i ($i = 1, 2, \dots, 69$): (a) The Fisher discriminant Ratio $F1(i)$; a high value of $F1(i)$ indicates that the feature is discriminant. (b) The ratio of the width of the overlap interval $F2(i)$; a low value of $F2(i)$ measure means that the feature can discriminate the samples of different classes. (c) The individual feature efficiency $F3(i)$; a high value of $F3(i)$ indicates a good efficiency. The horizontal dashed black lines correspond to the threshold values and the retained features are in red.

summarizes the selected features and their clinical meaning.

This result supports previous studies on biomechanical data and their association with knee pathologies. Indeed f_{62} , which corresponds to the ROM of the Internal-external rotation, has been identified as a characteristic of improvement following a total knee replacement surgery (Jones et al., 2006). Also, f_{26} , which is the mean of abduction-adduction angle during the stance phase, has been identified discriminant for knee osteoarthritis severity assessment.

The efficiency of the subset of selected features have been measured using the interclass distance measure (Table 3). This measure is higher when compared to interclass distance using the whole feature data set (1832.2 and 987.8 respectively) which show that the selected features discriminate better the two classes.

The statistical analysis reveals no differences in the general characteristics between the two groups (as described in Table 1), which means that these characteristics are not involved in the characterization of surgical and nonsurgical arthroplasty candidates.

Table 3: Surgical and nonsurgical interclass distances.

Data set	Inter class distance
Feature data set (69 biomechanical features)	987.8
Selected feature data set (12 retained biomechanical features)	1832.2

4 CONCLUSION

In this study, we developed a feature selection method for 3D knee kinematic data using statistical measures of class ambiguity. We investigated each feature taken individually using the Fisher discriminant ratio, volume of overlap region, feature efficiency. Within the original 69 biomechanical features extracted from the 3D kinematic signals, 12 features have been selected that contain pertinent information to characterize surgical vs nonsurgical arthroplasty subjects. This set of discriminant features can also help in future clinical studies to identify biomarkers for knee surgical arthroplasty candidate treatment.

In a subsequent study, the selected features will serve as input to build classification models to help discriminate automatically surgical from nonsurgical arthroplasty subjects.

ACKNOWLEDGEMENTS

This research was supported in part by the Natural Sciences and Engineering Research Council Grant (RGPIN-2015-03853) and the Canada Research Chair on Biomedical Data Mining (950-231214). The authors would like to thank Hilary Mac Donald and Tim Parlee for the kinematic data collection.

REFERENCES

- Astephen, J., Deluzio, K., Dunbar, M., Caldwell, G., and Hubley-Kozey, C. (2011). The association between knee joint biomechanics and neuromuscular control and moderate knee osteoarthritis radiographic and pain severity. *Osteoarthritis Cartilage*, 26(3):186–193.
- Bytyqi, D., Shabani, B., Lustig, S., Cheze, L., Karahoda Gjurgjeala, N., and Neyret, P. (2014). Gait knee kinematic alterations in medial osteoarthritis: three dimensional assessment. *Int. Orthop.*, 38(6):1191–1198.
- Casino, D., Martelli, S., and Zaffagnini, S. (2009). Knee stability before and after total and unicompartmental knee replacement: In vivo kinematic evaluation utilizing navigation. *Journal of Orthopaedic Research*, 27(2):202–207.
- Casino, D., Zaffagnini, S., and Martelli, S. (2008). Intraoperative evaluation of total knee replacement: kinematic assessment with a navigation system. *Knee Surgery, Sports Traumatology, Arthroscopy*, 17(4):369–373.
- Jones, L., Beynon, M., Holt, C., and Roy, S. (2006). An application of the Dempster-Shafer theory of evidence to the classification of knee function and detection of improvement due to total knee replacement surgery. *J Biomechanics*, 39(13):2512–2520.
- Lorena, A. C. and de Souto, M. C. P. (2015). *On Measuring the Complexity of Classification Problems*, pages 158–167. Springer International Publishing, Cham.
- Lustig, S., Magnussen, R., Cheze, L., and Neyret, P. (2012). The knee system: a review of the literature. *Knee Surg. Sport. Traumatol. Arthrosc.*, 20(4):633–638.
- Mezghani, N., Husse, S., Boivin, K., Turcot, K., Aissaoui, R., Hagemester, N., and de Guise, J. (2008). Identification of knee frontal plane kinematic patterns in normal gait by principal component analysis. *Journal of Mechanics in Medicine and Biology*, 13(3):r1230–1232.
- Mezghani, N., Ouakrim, Y., Fuentes, A., Mitiche, A., Whynot, S., Richardson, G., and M, D. (2016). Biomechanical signal classification of surgical and non-surgical candidates for knee arthroplasty. *The IEEE International Symposium on signal, Image, Video and Communication (ISIVC)*.
- Mezghani, N., Ouakrim, Y., Fuentes, A., Mitiche, A., Whynot, S., Richardson, G., and M, D. (2017). Mechanical biomarkers of medial compartment knee osteoarthritis diagnosis and severity grading: Discovery phase. *Journal of biomechanics*, 52(1):106–112.
- Mihalko, W., Ali, M., Phillips, M., Bayers-Thering, M., and KA, K. (2007). Passive knee kinematics before and after total knee arthroplasty. *The Journal of Arthroplasty*, 23(1):57–60.
- Seon, J., Park, J., Jeong, M., Jung, W., Park, K., Yoon, T., and EK, S. (2011). Correlation between preoperative and postoperative knee kinematics in total knee arthroplasty using cruciate retaining designs. *Int Orthopedic*, 35(4):515–520.